

Article

A Fluorescent Linear Conjugated Polymer Constructed from Pillararene and Anthracene

Dinghui Wang [†], Jun Wang [†], Yan Wang ^{*} and Yingwei Yang ^{*ID}

International Joint Research Laboratory of Nano-Micro Architecture Chemistry, College of Chemistry, Jilin University, 2699 Qianjin Street, Changchun 130012, China; wangdh19@mails.jlu.edu.cn (D.W.); junw19@mails.jlu.edu.cn (J.W.)

^{*} Correspondence: wangy2011@jlu.edu.cn (Y.W.); ywyang@jlu.edu.cn (Y.Y.)

[†] These authors contributed equally to this work.

Abstract: Over the past few years, conjugated polymers (CPs) have aroused much attention owing to their rigid conjugated structures, which can perform well in light harvesting and energy transfer and offer great potential in materials chemistry. In this article, we fabricate a new luminescent linear CP p(P[5](OTf)₂-co-9,10-dea) via the Sonogashira coupling of 9,10-diethynylanthracene and trifluoromethanesulfonic anhydride (OTf) modified pillar[5]arene, generating enhanced yellow-green fluorescence emission at around 552 nm. The reaction condition was screened to get a deeper understanding of this polymerization approach, resulting in an excellent yield as high as 92% ultimately. Besides the optical properties, self-assembly behaviors of the CP in low/high concentrations were studied, where interesting adjustable morphologies from tube to sheet were observed. In addition, the fluorescence performance and structural architecture can be disturbed by the host-guest reorganization between the host CP and the guest adiponitrile, suggesting great potential of this CP material in the field of sensing and detection.

Keywords: conjugated polymer; host-guest interaction; pillararene; supramolecular chemistry; light-emitting materials



Citation: Wang, D.; Wang, J.; Wang, Y.; Yang, Y. A Fluorescent Linear Conjugated Polymer Constructed from Pillararene and Anthracene. *Molecules* **2022**, *27*, 3162. <https://doi.org/10.3390/molecules27103162>

Academic Editor: Maksymilian Chruszcz

Received: 21 April 2022

Accepted: 14 May 2022

Published: 15 May 2022

Publisher's Note: MDPI stays neutral with regard to jurisdictional claims in published maps and institutional affiliations.



Copyright: © 2022 by the authors. Licensee MDPI, Basel, Switzerland. This article is an open access article distributed under the terms and conditions of the Creative Commons Attribution (CC BY) license (<https://creativecommons.org/licenses/by/4.0/>).

1. Introduction

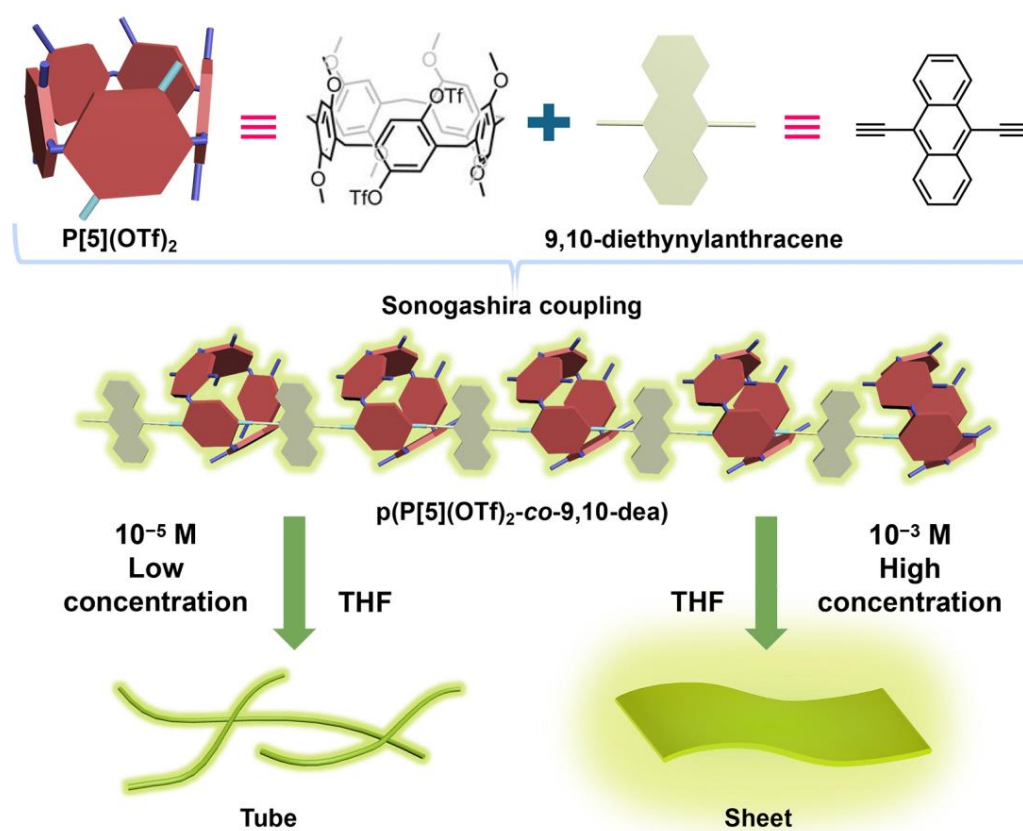
Compared with traditional flexible non-conjugated polymers and small conjugated molecules, conjugated polymers (CPs) containing rigid conjugated backbones have outstanding capability of light harvesting and energy transfer, favorable to the generation of luminescence, thus endowing widespread applications in electronic sensing devices, solar battery, and semiconductor materials [1–10]. Consequently, it is essential to work out facile and powerful strategies for obtaining promoted light-emitting CPs with high efficiency [11–17].

Supramolecular assemblies have been widely reported to assist in constructing CP-based artificial light-harvesting systems [18]. With the rapid development of supramolecular chemistry, various macrocyclic compounds with rigid structures have been designed and synthesized [19–23]. Benefiting from their facile synthesis, high yield, rigid cavity structures, and easy modification, pillararenes and their derivatives, as a relatively new class of synthetic macrocycles, have been widely applied for the design of high-performance fluorescent supramolecular polymeric materials [24–28], guaranteeing a variety of applications in fluorescence imaging [29,30], substance detection [31,32], electroluminescence materials [33–38], and fluorescence sensor [39–42]. For example, our group reported one conjugated macrocycle polymer (CMP) from tetraphenylethene (TPE) modified pillar[5]arene, which could be manufactured into a well-behaved fluorescence sensor to detect Fe³⁺ and 4-aminoazobenzene, suggesting promising potential for the removal of environmental pollutants [43]. In addition, the applications of CMP materials in catalysis, sensing, adsorption, and separation have been studied in detail [44–51]. However, common CMP

materials show limitations in solubility due to the strongly cross-linked structures, which leads to weak processability. To overcome this drawback, linear CPs containing pillararenes have been obtained through Suzuki coupling by Tang and coworkers [52]. Instead of covalently bonding with pillararenes, the guest TPE molecules were brought into the linear backbone successfully through the encapsulation of the host pillararenes. This system not only showed a highly efficient light-harvesting property with fluorescence enhancement but also promised excellent solubility in CHCl_3 /c-hexane. Our research group also reported two kinds of linear CPs constructed from terphenyl and diphenyl-pillararenes and their applications in photocatalysis on the basis of the enlarged visible-light absorption region and tunable optoelectronic properties [1].

To enrich the synthetic methods and stimulate the property improvement of CPs, several methods have been utilized to construct linear CPs, including Suzuki coupling [53], Heck reaction [54], Negishi coupling [55], Stille coupling [56], and Sonogashira coupling [57]. Benefiting from the co-catalysis of copper and palladium, Sonogashira coupling as one of the essential methods for the palladium-catalyzed coupling reaction of halogenated aryl compounds with terminal alkynes shows the advantages of high yields and mild reaction conditions, enabling the synthesis of linear CPs with good solubility and high machinability [58].

Herein, we fabricate a new linear fluorescent CP, $p(\text{P}[5](\text{OTf})_2\text{-co-9,10-dea})$, from the Sonogashira coupling of trifluoromethanesulfonic anhydride (OTf)-modified pillar[5]arene and 9,10-diethynylantracene containing alkynyl, which could generate strengthened yellow-green fluorescence emission at around 552 nm in THF (Scheme 1). Notably, the best reaction conditions of Sonogashira coupling were selected by adopting the control variable method. Moreover, tunable fluorescence intensity and morphologies could be realized by varying the solution concentration of $p(\text{P}[5](\text{OTf})_2\text{-co-9,10-dea})$ or the guest adiponitrile.



Scheme 1. Schematic representation of the linear fluorescent CP, $p(\text{P}[5](\text{OTf})_2\text{-co-9,10-dea})$, and its tunable morphology under different concentrations.

2. Results and Discussion

2.1. Polymerization

According to the previously published procedures, two reactants, that is P[5](OTf)₂ and 9,10-diethynylantracene, and the CP (p(P[5](OTf)₂-co-9,10-dea) were synthesized and characterized by ¹H nuclear magnetic resonance (¹H NMR) and ¹³C NMR (Scheme S1 and Figures S1–S8) [59,60]. Then the key parameters of Sonogashira coupling, involving solvent, reaction time, temperature, and the feed ratio of catalyst, were profoundly studied to achieve the highest polymerization yield of this new system; the detailed contents are as follows.

Firstly, four kinds of organic solvents were selected according to the reported Sonogashira coupling systems to investigate the solvent effect [61]. As shown in Table 1, the solvents all ensured the polymerization in good progress, among which THF was identified as the most suitable one for the polymerization, allowing the highest yield up to 92% (Table 1, Entry 2).

Table 1. Solvent effect on the polymerization carried out under N₂ atmosphere for 24 h in the presence of CuI and Et₃N. T = 90 °C; [P[5](OTf)₂] = [9,10-diethynylantracene] = 0.30 M; [Pd(PPh₃)₂Cl₂] = 0.02 M; [PPh₃] = 0.03 M; [CuI] = 0.04 M; Et₃N = 0.6 mL.

Entry	Solvent	Yield (%)
1	CHCl ₃	88
2	THF	92
3	DMF	72
4	CH ₂ Cl ₂	74

Then, the influence of reaction time was systematically discussed in the most optimized solvent THF (Table 2). The polymeric product started to yield after 8 h with a conversion rate of 27% (Table 2, Entry 1). Prolonging the reaction time to 24 h kept raising the yield to 92% (Table 2, Entries 2–5). However, further increased duration of polymerization to more than 24 h was not favorable for the formation of the CP because the decreased activity of the catalyst caused by the complex of CuI and 9,10-diethynylantracene resulted in reduced yields (Table 2, Entries 6 and 7) [62]. Therefore, 24 h was preferred as the optimum reaction time in subsequent studies.

Table 2. Time course of the polymerization carried out under N₂ atmosphere in the presence of CuI and Et₃N in THF. T = 90 °C; [P[5](OTf)₂] = [9,10-diethynylantracene] = 0.30 M; [Pd(PPh₃)₂Cl₂] = 0.02 M; [PPh₃] = 0.03 M; [CuI] = 0.04 M; Et₃N = 0.6 mL.

Entry	Reaction Time (h)	Yield (%)
1	8	27
2	10	43
3	11	60
4	12	77
5	24	92
6	36	91
7	48	82

Afterward, the temperature effect on the polymerization was investigated. Due to the bad reactivity of substituted aromatic hydrocarbons at low temperatures (≤ 60 °C), it is necessary to elevate the chemical reactivity by increasing the reaction temperature (Table 3, Entries 1 and 2). Upon raising the temperature to 70 °C, the CP started to generate with a yield of 18% (Table 3, Entry 3). Upon increasing the temperature to 90 °C, further production increment was achieved (92%, Table 3, Entries 4–7). However, when conducting the reaction at 100 °C, a slightly reduced yield was observed (Table 3, Entry 8). We rationally inferred that this negative result ascribes to the unnecessary side reactions in high-temperature

environments [63]. Since too high and too low temperatures are not favorable for the Sonogashira coupling, we chose 90 °C as the ideal reaction temperature.

Table 3. Temperature effect on the polymerization carried out under N₂ atmosphere for 24 h in the presence of CuI and Et₃N in THF. [P[5](OTf)₂] = [9,10-diethynylanthracene] = 0.30 M; [Pd(PPh₃)₂Cl₂] = 0.02 M; [PPh₃] = 0.03 M; [CuI] = 0.04 M; Et₃N = 0.6 mL.

Entry	Reaction Temperature (°C)	Yield (%)
1	25	/
2	60	/
3	70	18
4	75	34
5	80	59
6	85	79
7	90	92
8	100	89

Last but not least, the amount of CuI as the co-catalyst is vital to the reduction reaction of the palladium catalyst in the Sonogashira coupling. Nevertheless, excessive CuI results in the complex formation with 9,10-diethynylanthracene, minimizing reactant concentration. As we assumed, the polymer p(P[5](OTf)₂-co-9,10-dea) engendered only in 0.03 M (79%), 0.04 M (92%), and 0.05 M (71%) (Table 4), where 0.04 M CuI presents the best co-catalyst concentration for the following polymerization.

Table 4. Effect of catalyst loading on the polymerization carried out under N₂ atmosphere for 24 h in the presence of CuI and Et₃N in THF. T = 90 °C; [P[5](OTf)₂] = [9,10-diethynylanthracene] = 0.30 M; [Pd(PPh₃)₂Cl₂] = 0.02 M; [PPh₃] = 0.03 M; Et₃N = 0.6 mL.

Entry	CuI (M)	Yield (%)
1	0.10	/
2	0.05	79
3	0.04	92
4	0.03	71
5	0.02	/
6	0.01	/

2.2. Structural Characterization

Compared with the previously reported CMP materials and heteroatoms-containing CPs, the new linear p(P[5](OTf)₂-co-9,10-dea) obtained under the optimized reaction condition combines the superiorities of conjugate rigid plane structure and good solubility, which enables its characterization in solution. Firstly, we characterized the number of average molecular weight (M_n) and the polymer dispersity index (PDI) by gel permeation chromatography (GPC). As illustrated in Figure 1a and Figure S9, M_n and PDI were calculated to be 4103 and 1.46, respectively, revealing 4–5 repeating units in one single chain of the resulting CP. This is in good agreement with the literature reports that the strengthened steric hindrance effect of reactants always results in short chains [64–67]. The M_n calculated from the ¹H NMR spectrum of p(P[5](OTf)₂-co-9,10-dea) is 3798, which coincides well with the GPC result. Then, X-ray diffraction (XRD) pattern showed the disappearance of P[5](OTf)₂ peaks. New peaks emerged in p(P[5](OTf)₂-co-9,10-dea), indicating its crystalline structure (Figure 1b).

The 2D rotating frame Overhauser effect spectroscopy nuclear magnetic resonance (2D ROESY NMR) experiment of p(P[5](OTf)₂-co-9,10-dea) supports the correlations between the methoxy moieties at around 3.44–3.93 ppm (H₁) and the phenyl protons at around 6.50–6.93 ppm (H_a), demonstrating the strong intermolecular interactions between the polymer chains (Figure 2).

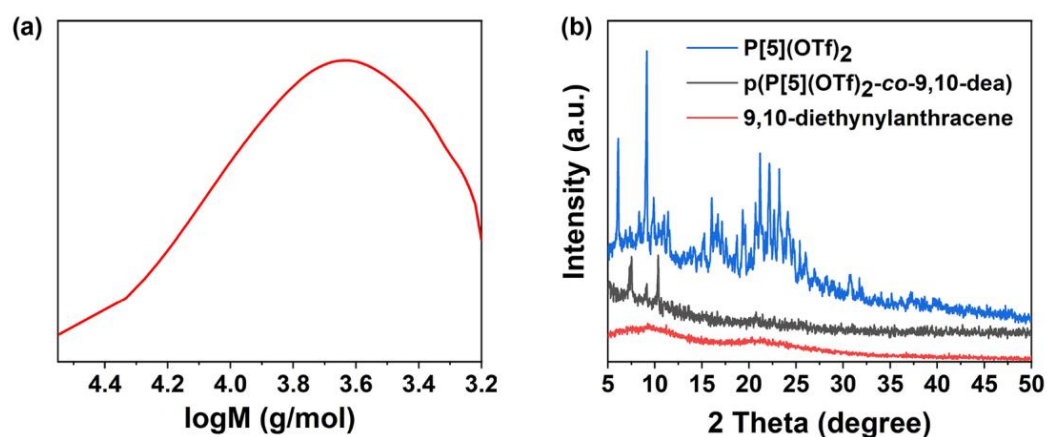


Figure 1. (a) GPC trace of $p(\text{P}[5](\text{OTf})_2\text{-co-9,10-dea})$. (b) XRD patterns of $\text{P}[5](\text{OTf})_2$ (blue), $p(\text{P}[5](\text{OTf})_2\text{-co-9,10-dea})$ (black), and 9,10-diethynylantracene (red).

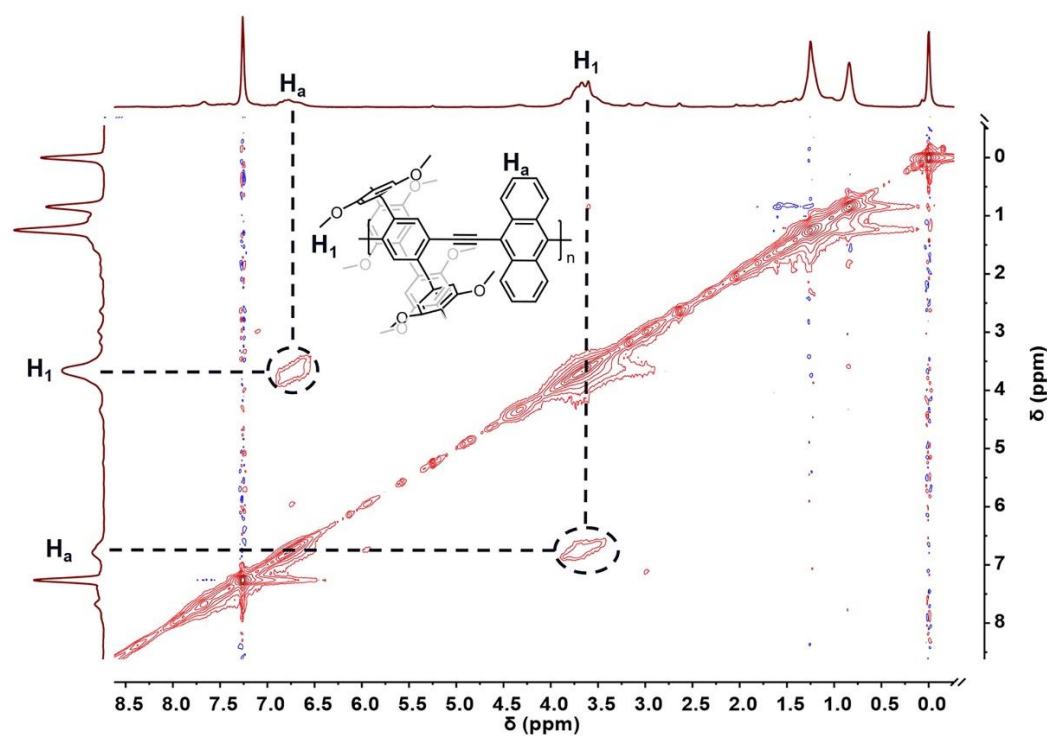


Figure 2. Two-dimensional ROESY spectrum (600 MHz, CDCl_3 , 298 K) of $p(\text{P}[5](\text{OTf})_2\text{-co-9,10-dea})$.

2.3. Fluorescence Properties

As the reaction proceeded, the conjugated structure was further extended, which increased electron delocalization and reduced the energy required for electron transitions, thus resulting in the redshift of the ultraviolet-visible (UV-vis) absorption band and the corresponding fluorescence emission band to 480 nm and 552 nm, respectively (Figure 3a,b and Figures S10–S12). When increasing the CP concentration in THF, the UV-vis absorption and fluorescence intensities were all raised. Nevertheless, after introducing the poor solvent H_2O to the solution, fluorescence intensity decreased significantly, revealing quenching from π - π stacking of the polymeric dye (Figure S13) [68]. Additionally, a reduced lifetime of about 1.11 ns and promoted quantum yield of around 9.40% of $p(\text{P}[5](\text{OTf})_2\text{-co-9,10-dea})$ solution were produced, which is conducive to the construction of efficient short-frequency emission fluorescent materials (Figure 3c,d, and Figures S14 and S15).

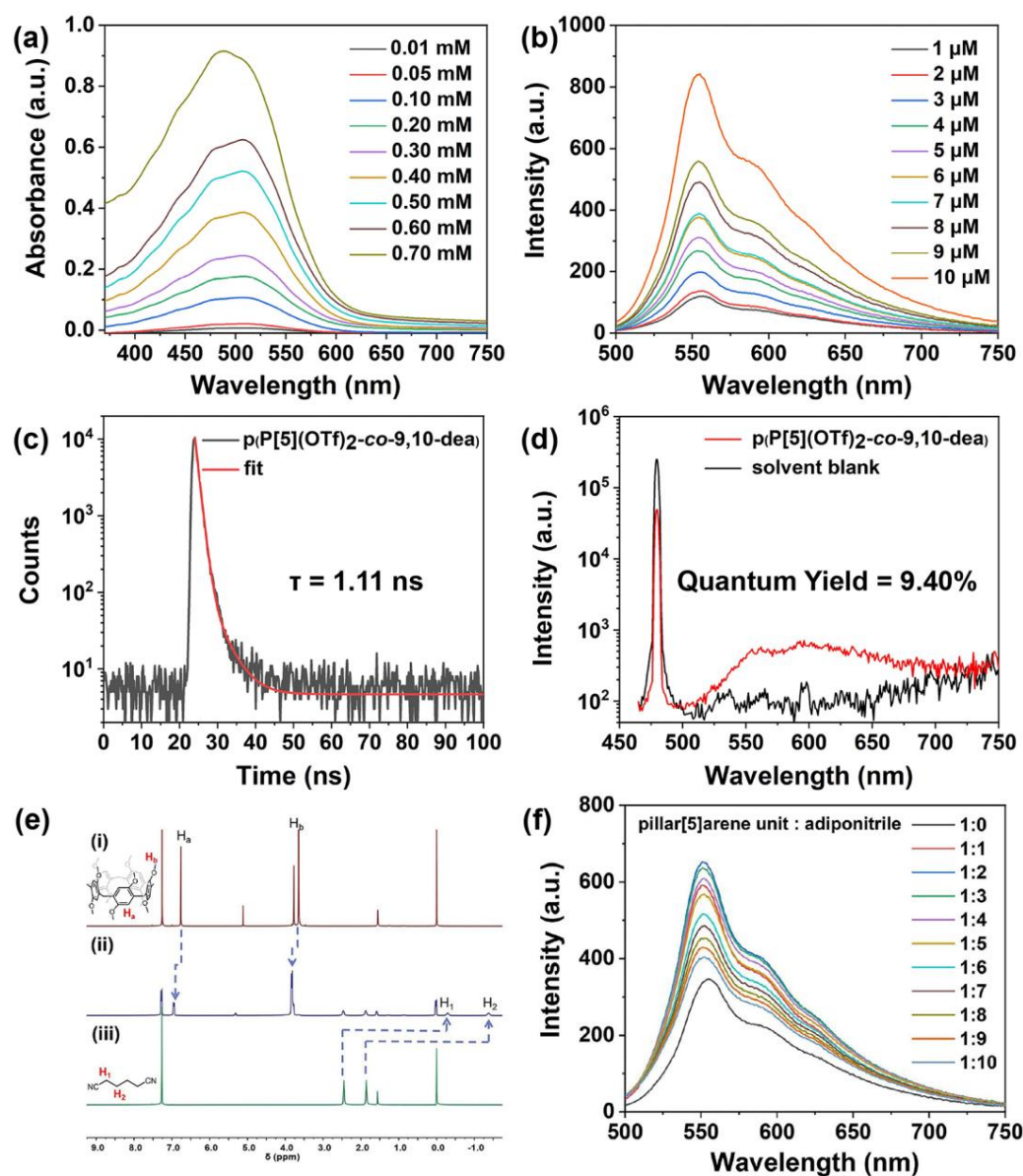


Figure 3. (a) The UV-vis absorption spectra and (b) fluorescence spectra of p(P[5](OTf)₂-co-9,10-dea) CP in THF with increasing concentration (slit widths: ex. 5 nm, em. 3 nm; 25 °C). (c) Fluorescence decay profile and (d) quantum yield of p(P[5](OTf)₂-co-9,10-dea) (solvent: THF, $\lambda_{\text{ex}} = 480$ nm; [pillar[5]arene unit] = 10^{-5} M, 25 °C). (e) Characterization of the host–guest interactions between pillar[5]arenes and adiponitrile guests by NMR spectroscopy. ¹H NMR spectra (400 MHz, CDCl₃, 298 K) of (i) DMP[5]A (5×10^{-3} M), (ii) the equimolar mixture of DMP[5]A (5×10^{-3} M) and adiponitrile (5×10^{-3} M), (iii) adiponitrile (5×10^{-3} M). (f) Fluorescent emission spectra of p(P[5](OTf)₂-co-9,10-dea) in THF with different ratio of adiponitrile ($\lambda_{\text{ex}} = 480$ nm; $\lambda_{\text{em}} = 552$ nm; slit widths: ex. 5 nm, em. 3 nm; 25 °C).

The current pillar[5]arenes with an intrinsic π -electron-rich cavity in the CP chain endow the selective recognition to the cyano group based on the host–guest interaction (Figure 3e). The introduction of suitable guest molecules undoubtedly affects the fluorescence emission of CP. The fluorescence spectra with different ratios of adiponitrile containing cyano groups at chain ends were collected (Figures 3f and S16), which revealed an appreciable nonlinear relationship between the fluorescence intensity and the guest–host ratio within the range from 2:1 to 20:1, offering new possibilities for the application of sensing and detection.

2.4. Tunable Morphologies Induced by Concentration

To comprehensively understand this new CP, we continue to investigate its assembly structures at different concentrations by the scanning electron microscope (SEM) and dynamic light scattering (DLS) experiments. At a low concentration of 1×10^{-5} M, p(P[5](OTf)_{2-co-9,10-dea}) assembled into a linear long-chain structure of about 970 μm (Figure 4a). The narrow distributed hydrodynamic radius was found to be 615 nm, demonstrating the good dispersibility and stability of this CP in THF (Figure 4b). As shown in Figure 4c, when increased the concentration to 1×10^{-3} M, p(P[5](OTf)_{2-co-9,10-dea}) changed its self-assembled structure to a wrinkled film due to the amplified intermolecular interactions as we characterized above. This interesting transformation provides an idea for building fluorescent systems with controllable structures. In addition, the structures were disturbed after the combination of p(P[5](OTf)_{2-co-9,10-dea}) and adiponitrile. The formation of the supramolecular polymer limited the aggregation of the CP with planar structure, forming into irregular blocks (Figure 4d).

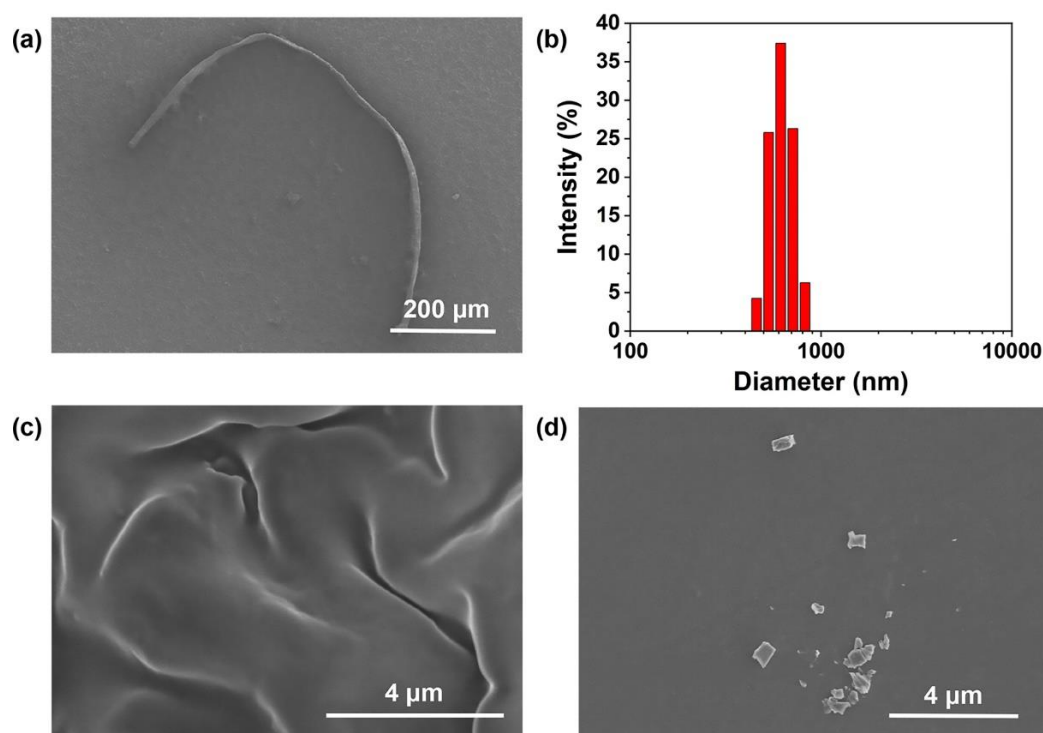


Figure 4. (a) SEM image and (b) hydrodynamic size of p(P[5](OTf)_{2-co-9,10-dea}) in THF, [pillar[5]arene unit] = 10^{-5} M. (c) SEM image of p(P[5](OTf)_{2-co-9,10-dea}) in THF ([pillar[5]arene unit] = 10^{-3} M) and (d) adiponitrile and p(P[5](OTf)_{2-co-9,10-dea}) in THF ([pillar[5]arene unit]: [adiponitrile] = 1:10).

3. Materials and Methods

3.1. Materials

All the reagents and solvents were purchased from commercial sources and used as received unless otherwise noted. Deionized water, purified by Experimental Water System (Lab-UV-20), was used in the relevant experiments.

3.2. Physical Characterization and Techniques

¹H NMR and ¹³C NMR spectra were recorded on a Bruker Avance 400 MHz spectrometer, and 2D ROESY NMR spectra were recorded on a Bruker AVANCEIII 600 MHz instrument. UV-vis spectra were recorded on a Shimadzu UV-2550 instrument. XRD measurements were carried out on a PANalytical B.V. Empyrean powder diffractometer. GPC was performed on a Malvern instrument, equipped with a PLgel MIXED guard column followed

by a PLgel MIXED guard column (molecular weight range 2.0×10^2 – 4.0×10^5 g/mol), column thermostated to 60 °C, and calibrated by linear polystyrene standards. THF was used as the eluent at a flow of 0.8 mL/min at 60 °C. The fluorescent experiments were conducted on an RF-5301 spectrofluorophotometer (Shimadzu Corporation, Kyoto, Japan). The time-resolved fluorescence decay curves and fluorescence quantum yields were obtained on an FLS920 instrument (Edinburgh Instrument, Livingston, UK). DLS was obtained on a Zetasizer Nano ZS instrument. Scanning electron microscope (SEM) images were obtained on a HITACHI-SU8082 instrument.

4. Conclusions

In this work, we successfully designed and prepared a new type of CP with linear structure and good solubility via the Sonogashira coupling, achieving a polymerization yield as high as 92% after optimizing the reaction parameters. Notably, promoted red-shifted yellow-green fluorescence at around 552 nm was harvested in THF. When regulating the concentration/adding the guest adiponitrile, diverse fluorescence intensity and self-assembly structures from line to film/irregular blocks were attained when regulating the concentration/adding the guest adiponitrile. In general, this fluorescent linear CP with concentration/adiponitrile-dependent luminescence properties and self-assembly characteristics is appropriate for sensing and available in the fabrication of well-performing light harvesting and energy transfer pure organic materials with controllable structures.

Supplementary Materials: The following supporting information can be downloaded at: <https://www.mdpi.com/article/10.3390/molecules27103162/s1>, Figures S1–S9: Synthetic routes and structural characterization of compounds and polymer; Figures S10–S17: The luminescence spectra of materials.

Author Contributions: Conceptualization, D.W.; Methodology, D.W.; Validation, D.W., J.W. and Y.W.; Formal Analysis, D.W., J.W. and Y.W.; Writing—original Draft Preparation, D.W. and J.W.; Writing—review and Editing, Y.Y.; Supervision, Y.W. and Y.Y. All authors have read and agreed to the published version of the manuscript.

Funding: This research was funded by National Natural Science Foundation of China (grant No. 21871108).

Institutional Review Board Statement: Not applicable.

Informed Consent Statement: Not applicable.

Data Availability Statement: Not applicable.

Conflicts of Interest: The authors declare no conflict of interest.

Sample Availability: Samples of the compounds are not available from the authors.

References

1. Li, Z.; Li, L.; Wang, Y.; Yang, Y.-W. Pillararene-enriched linear conjugated polymer materials with thiazolo [5,4-d]thiazole linkages for photocatalysis. *Chem. Commun.* **2021**, *57*, 6546–6549. [[CrossRef](#)] [[PubMed](#)]
2. Cui, W.; Tang, H.; Xu, L.X.; Wang, L.Y.; Meier, H.; Cao, D.R. Pillar[5] arene-Diketopyrrolopyrrole Fluorescent Copolymer: A Promising Recognition and Adsorption Material for Adiponitrile by Selective Formation of a Conjugated Polypseudorotaxane. *Macromol. Rapid Commun.* **2017**, *38*, 1700161. [[CrossRef](#)] [[PubMed](#)]
3. Ma, Y.J.; Chen, L.; Li, C.; Mullen, K. A fishing rod-like conjugated polymer bearing pillar[5] arenes. *Chem. Commun.* **2016**, *52*, 6662–6664. [[CrossRef](#)] [[PubMed](#)]
4. Hou, J.H.; Huo, L.J.; He, C.; Yang, C.H.; Li, Y.F. Synthesis and Absorption Spectra of Poly(3-(phenylenevinyl)thiophene)s with Conjugated Side Chains. *Macromolecules* **2006**, *39*, 594–603. [[CrossRef](#)]
5. Hou, J.H.; Yang, C.H.; He, C.; Li, Y.F. Poly [3-(5-octyl-thienylene-vinyl)-thiophene]: A Side-chain Conjugated Polymer with Very Broad Absorption Band. *Chem. Commun.* **2006**, *8*, 871–873. [[CrossRef](#)]
6. Li, Z.; Yang, Y.W. Macrocyclic-Based Porous Organic Polymers for Separation, Sensing, and Catalysis. *Adv. Mater.* **2022**, *34*, e2107401. [[CrossRef](#)]
7. Li, Z.; Yang, Y.-W. Conjugated macrocyclic polymers. *Polym. Chem.* **2021**, *12*, 4613–4620. [[CrossRef](#)]
8. Lou, X.-Y.; Yang, Y.-W. Pyridine-Conjugated Pillar[5] arene: From Molecular Crystals of Blue Luminescence to Red-Emissive Coordination Nanocrystals. *J. Am. Chem. Soc.* **2021**, *143*, 11976–11981. [[CrossRef](#)]

9. Yu, D.X. Light-emitting devices with conjugated polymers. *Int. J. Mol. Sci.* **2011**, *12*, 1575–1594. [[CrossRef](#)]
10. Tuncel, D.; Demir, H.V. Conjugated polymer nanoparticles. *Nanoscale* **2010**, *2*, 484–494. [[CrossRef](#)]
11. Wasielewski, M.R. Self-Assembly Strategies for Integrating Light Harvesting and Charge Separation in Artificial Photosynthetic Systems. *Acc. Chem. Res.* **2009**, *42*, 1910–1921. [[CrossRef](#)] [[PubMed](#)]
12. Song, N.; Lou, X.-Y.; Hou, W.; Wang, C.-Y.; Wang, Y.; Yang, Y.-W. Pillararene-Based Fluorescent Supramolecular Systems: The Key Role of Chain Length in Gelation. *Macromol. Rapid Commun.* **2018**, *39*, e1800593. [[CrossRef](#)] [[PubMed](#)]
13. Wang, X.-H.; Song, N.; Hou, W.; Wang, C.-Y.; Wang, Y.; Tang, J.; Yang, Y.-W. Efficient Aggregation-Induced Emission Manipulated by Polymer Host Materials. *Adv. Mater.* **2019**, *31*, e1903962. [[CrossRef](#)] [[PubMed](#)]
14. Wu, M.X.; Wang, X.; Yang, Y.W. Polymer Nanoassembly as Delivery Systems and Anti-Bacterial Toolbox: From PGMA to MSN@PGMA. *Chem. Rec.* **2018**, *18*, 45–54. [[CrossRef](#)]
15. Li, Q.Y.; Wu, Y.H.; Lu, H.G.; Wu, X.S.; Chen, S.; Song, N.; Yang, Y.-W.; Gao, H. Construction of Supramolecular Nanoassembly for Responsive Bacterial Elimination and Effective Bacterial Detection. *ACS Appl. Mater. Interfaces* **2017**, *9*, 10180–10189. [[CrossRef](#)]
16. Lou, X.Y.; Song, N.; Yang, Y.W. Fluorescence Resonance Energy Transfer Systems in Supramolecular Macrocyclic Chemistry. *Molecules* **2017**, *22*, 1640. [[CrossRef](#)]
17. Song, N.; Lou, X.-Y.; Yu, H.; Weiss, P.S.; Tang, B.Z.; Yang, Y.-W. Pillar[5] arene-based tunable luminescent materials via supramolecular assembly-induced Förster resonance energy transfer enhancement. *Mater. Chem. Front.* **2020**, *4*, 950–956. [[CrossRef](#)]
18. Guo, S.W.; Song, Y.S.; He, Y.L.; Hu, X.Y.; Wang, L.Y. Highly Efficient Artificial Light-Harvesting Systems Constructed in Aqueous Solution Based on Supramolecular Self-Assembly. *Angew. Chem. Int. Ed. Engl.* **2018**, *57*, 3163–3167. [[CrossRef](#)]
19. Wu, J.-R.; Yang, Y.-W. New opportunities in synthetic macrocyclic arenes. *Chem. Commun.* **2019**, *55*, 1533–1543. [[CrossRef](#)]
20. Xia, D.Y.; Wang, P.; Ji, X.F.; Khashab, N.M.; Sessler, J.L.; Huang, F.H. Functional Supramolecular Polymeric Networks: The Marriage of Covalent Polymers and Macrocyclic-Based Host-Guest Interactions. *Chem. Rev.* **2020**, *120*, 6070–6123. [[CrossRef](#)]
21. Ogoshi, T.; Kanai, S.; Fujinami, S.H.; Yamagishi, T.; Nakamoto, Y. para-Bridged Symmetrical Pillar[5] arenes: Their Lewis Acid Catalyzed Synthesis and Host–Guest Property. *J. Am. Chem. Soc.* **2008**, *130*, 5022–5023. [[CrossRef](#)] [[PubMed](#)]
22. Shao, L.; Pan, Y.T.; Hua, B.; Xu, S.D.; Yu, G.C.; Wang, M.B.; Liu, B.; Huang, F.H. Constructing Adaptive Photosensitizers via Supramolecular Modification Based on Pillararene Host-Guest Interactions. *Angew. Chem. Int. Ed. Engl.* **2020**, *59*, 11779–11783. [[CrossRef](#)] [[PubMed](#)]
23. Li, Z.; Yang, Y.-W. Functional Materials with Pillarene Struts. *Acc. Mater. Res.* **2021**, *2*, 292–305. [[CrossRef](#)]
24. Tan, L.-L.; Yang, Y.-W. Molecular recognition and self-assembly of pillarenes. *J. Incl. Phenom. Macrocycl. Chem.* **2014**, *81*, 13–33. [[CrossRef](#)]
25. Ogoshi, T.; Yamafuji, D.; Aoki, T.; Yamagishi, T.A. Photoreversible transformation between seconds and hours time-scales: Threading of pillar[5] arene onto the azobenzene-end of a viologen derivative. *J. Org. Chem.* **2011**, *76*, 9497–9503. [[CrossRef](#)]
26. Tuo, W.; Sun, Y.; Lu, S.; Li, X.P.; Sun, Y.; Stang, P.J. Pillar[5]arene-Containing Metallacycles and Host-Guest Interaction Caused Aggregation-Induced Emission Enhancement Platforms. *J. Am. Chem. Soc.* **2020**, *142*, 16930–16934. [[CrossRef](#)]
27. Lan, S.; Liu, Y.M.; Shi, K.J.; Ma, D. Acetal-Functionalized Pillar[5] arene: A pH-Responsive and Versatile Nanomaterial for the Delivery of Chemotherapeutic Agents. *ACS Appl. Bio Mater.* **2020**, *3*, 2325–2333. [[CrossRef](#)]
28. Strutt, N.L.; Fairen-Jimenez, D.; Iehl, J.; Lalonde, M.B.; Snurr, R.Q.; Farha, O.K.; Hupp, J.T.; Stoddart, J.F. Incorporation of an A1/A2-difunctionalized pillar[5] arene into a metal-organic framework. *J. Am. Chem. Soc.* **2012**, *134*, 17436–17439. [[CrossRef](#)]
29. Wang, G.; Yin, H.; Yin Ng, J.C.; Cai, L.P.; Li, J.; Tang, B.Z.; Liu, B. Polyethyleneimine-grafted hyperbranched conjugated polyelectrolytes: Synthesis and imaging of gene delivery. *Polym. Chem.* **2013**, *4*, 5297–5304. [[CrossRef](#)]
30. Deng, H.Q.; Han, T.; Zhao, E.G.; Kwok, R.T.K.; Lam, J.W.Y.; Tang, B.Z. Multicomponent Click Polymerization: A Facile Strategy toward Fused Heterocyclic Polymers. *Macromolecules* **2016**, *49*, 5475–5483. [[CrossRef](#)]
31. Liu, Y.; Lin, F.X.; Feng, Y.; Liu, X.Q.; Wang, L.; Yu, Z.Q.; Tang, B.Z. Shape-Persistent pi-Conjugated Macrocycles with Aggregation-Induced Emission Property: Synthesis, Mechanofluorochromism, and Mercury(II) Detection. *ACS Appl. Mater. Interfaces* **2019**, *11*, 34232–34240. [[CrossRef](#)] [[PubMed](#)]
32. Shao, L.; Sun, J.F.; Hua, B.; Huang, F.H. An AIEE fluorescent supramolecular cross-linked polymer network based on pillar[5] arene host-guest recognition: Construction and application in explosive detection. *Chem. Commun.* **2018**, *54*, 4866–4869. [[CrossRef](#)] [[PubMed](#)]
33. Huang, J.; Jiang, Y.B.; Yang, J.; Tang, R.L.; Xie, N.; Li, Q.Q.; Kwok, H.S.; Tang, B.Z.; Li, Z. Construction of efficient blue AIE emitters with triphenylamine and TPE moieties for non-doped OLEDs. *J. Mater. Chem. C* **2014**, *2*, 2028–2036. [[CrossRef](#)]
34. Zhao, Z.J.; Lam, J.W.Y.; Tang, B.Z. Tetraphenylethene: A versatile AIE building block for the construction of efficient luminescent materials for organic light-emitting diodes. *J. Mater. Chem.* **2012**, *22*, 23726–23740. [[CrossRef](#)]
35. Yu, Y.; Xu, Z.; Zhao, Z.; Zhang, H.; Ma, D.; Lam, J.W.Y.; Qin, A.; Tang, B.Z. In Situ Generation of Red-Emissive AIEgens from Commercial Sources for Nondoped OLEDs. *ACS Omega* **2018**, *3*, 16347–16356. [[CrossRef](#)] [[PubMed](#)]
36. Yao, H.; Ning, Y.; Jesson, C.P.; He, J.; Deng, R.H.; Tian, W.; Armes, S.P. Using Host–Guest Chemistry to Tune the Kinetics of Morphological Transitions Undertaken by Block Copolymer Vesicles. *ACS Macro Lett.* **2017**, *6*, 1379–1385. [[CrossRef](#)]
37. Li, Y.W.; Dong, Y.H.; Miao, X.R.; Ren, Y.L.; Zhang, B.L.; Wang, P.P.; Yu, Y.; Li, B.; Isaacs, L.; Cao, L.P. Shape-Controllable and Fluorescent Supramolecular Organic Frameworks Through Aqueous Host-Guest Complexation. *Angew. Chem. Int. Ed. Engl.* **2018**, *57*, 729–733. [[CrossRef](#)]

38. Huo, M.; Xu, Z.Y.; Zeng, M.; Chen, P.Y.; Liu, L.; Yan, L.T.; Wei, Y.; Yuan, J.Y. Controlling Vesicular Size via Topological Engineering of Amphiphilic Polymer in Polymerization-Induced Self-Assembly. *Macromolecules* **2017**, *50*, 9750–9759. [[CrossRef](#)]
39. Dong, W.H.; Wu, H.Q.; Chen, M.; Shi, Y.; Sun, J.Z.; Qin, A.J.; Tang, B.Z. Anionic conjugated polytriazole: Direct preparation, aggregation-enhanced emission, and highly efficient Al³⁺ sensing. *Polym. Chem.* **2016**, *7*, 5835–5839. [[CrossRef](#)]
40. Xu, L.G.; Hu, R.R.; Tang, B.Z. Room Temperature Multicomponent Polymerizations of Alkynes, Sulfonyl Azides, and Iminophosphorane toward Heteroatom-Rich Multifunctional Poly(phosphorus amidine)s. *Macromolecules* **2017**, *50*, 6043–6053. [[CrossRef](#)]
41. Li, B.; He, T.; Shen, X.; Tang, D.T.; Yin, S.C. Fluorescent supramolecular polymers with aggregation induced emission properties. *Polym. Chem.* **2019**, *10*, 796–818. [[CrossRef](#)]
42. Lou, X.Y.; Song, N.; Yang, Y.W. A stimuli-responsive pillar[5] arene-based hybrid material with enhanced tunable multicolor luminescence and ion-sensing ability. *Natl. Sci. Rev.* **2021**, *8*, nwaa281. [[CrossRef](#)] [[PubMed](#)]
43. Li, X.; Li, Z.; Yang, Y.-W. Tetraphenylethylene-Interweaving Conjugated Macrocyclic Polymer Materials as Two-Photon Fluorescence Sensors for Metal Ions and Organic Molecules. *Adv. Mater.* **2018**, *30*, e1800177. [[CrossRef](#)] [[PubMed](#)]
44. Li, Y.H.; Fang, Y.H.; Gao, W.Q.; Guo, X.J.; Zhang, X.M. Porphyrin-Based Porous Organic Polymer as Peroxidase Mimics for Sulfide-Ion Colorimetric Sensing. *ACS Sustain. Chem. Eng.* **2020**, *8*, 10870–10880. [[CrossRef](#)]
45. Talapaneni, S.N.; Kim, D.; Barin, G.; Buyukcakir, O.; Je, S.H.; Coskun, A. Pillar[5] arene Based Conjugated Microporous Polymers for Propane/Methane Separation through Host–Guest Complexation. *Chem. Mater.* **2016**, *28*, 4460–4466. [[CrossRef](#)]
46. Chen, R.F.; Shi, J.L.; Ma, Y.; Lin, G.Q.; Lang, X.J.; Wang, C. Designed Synthesis of a 2D Porphyrin-Based sp² Carbon-Conjugated Covalent Organic Framework for Heterogeneous Photocatalysis. *Angew. Chem. Int. Ed. Engl.* **2019**, *58*, 6430–6434. [[CrossRef](#)]
47. Li, Z.; Li, X.; Yang, Y.W. Conjugated Macrocyclic Polymer Nanoparticles with Alternating Pillarenes and Porphyrins as Struts and Cyclic Nodes. *Small* **2019**, *15*, 1805509. [[CrossRef](#)]
48. Dai, D.H.; Yang, J.; Zou, Y.C.; Wu, J.R.; Tan, L.L.; Wang, Y.; Li, B.; Lu, T.; Wang, B.; Yang, Y.W. Macrocyclic Arenes-Based Conjugated Macrocyclic Polymers for Highly Selective CO₂ Capture and Iodine Adsorption. *Angew. Chem. Int. Ed. Engl.* **2021**, *60*, 8967–8975. [[CrossRef](#)]
49. Qiang, H.; Chen, T.; Wang, Z.; Li, W.Q.; Guo, Y.Z.; Yang, J.; Jia, X.S.; Yang, H.; Hu, W.B.; Wen, K. Pillar[5] arene based conjugated macrocyclic polymers with unique photocatalytic selectivity. *Chin. Chem. Lett.* **2020**, *31*, 3225–3229. [[CrossRef](#)]
50. Li, M.H.; Lou, X.Y.; Yang, Y.W. Pillararene-based molecular-scale porous materials. *Chem. Commun.* **2021**, *57*, 13429–13447. [[CrossRef](#)]
51. Chen, W.B.; Chen, P.; Zhang, G.; Xing, G.L.; Feng, Y.; Yang, Y.W.; Chen, L. Macrocyclic-derived hierarchical porous organic polymers: Synthesis and applications. *Chem. Soc. Rev.* **2021**, *50*, 11684–11714. [[CrossRef](#)] [[PubMed](#)]
52. Xu, L.X.; Wang, Z.Y.; Wang, R.R.; Wang, L.Y.; He, X.W.; Jiang, H.F.; Tang, H.; Cao, D.R.; Tang, B.Z. A Conjugated Polymeric Supramolecular Network with Aggregation-Induced Emission Enhancement: An Efficient Light-Harvesting System with an Ultrahigh Antenna Effect. *Angew. Chem. Int. Ed. Engl.* **2020**, *59*, 9908–9913. [[CrossRef](#)] [[PubMed](#)]
53. Kadu, B.S. Suzuki–Miyaura cross coupling reaction: Recent advancements in catalysis and organic synthesis. *Catal. Sci. Technol.* **2021**, *11*, 1186–1221. [[CrossRef](#)]
54. Kurandina, D.; Chuentragool, P.; Gevorgyan, V. Transition-Metal-Catalyzed Alkyl Heck-Type Reactions. *Synthesis* **2019**, *51*, 985–1005. [[CrossRef](#)]
55. Huo, S.Q.; Mroz, R.; Carroll, J. Negishi coupling in the synthesis of advanced electronic, optical, electrochemical, and magnetic materials. *Org. Chem. Front.* **2015**, *2*, 416–445. [[CrossRef](#)]
56. Cordovilla, C.; Bartolomé, C.; Martínez-Ilduya, J.M.; Espinet, P. The Stille Reaction, 38 Years Later. *ACS Catal.* **2015**, *5*, 3040–3053. [[CrossRef](#)]
57. Nasrollahzadeh, M.; Motahharifar, N.; Ghorbannezhad, F.; Soheili Bidgoli, N.S.; Baran, T.; Varma, R.S. Recent advances in polymer supported palladium complexes as (nano)catalysts for Sonogashira coupling reaction. *Mol. Catal.* **2020**, *480*, 110645. [[CrossRef](#)]
58. Zhang, H.C.; Han, J.; Li, C. Pillararene-based conjugated porous polymers. *Polym. Chem.* **2021**, *12*, 2808–2824. [[CrossRef](#)]
59. Li, Q.; Zhu, H.T.Z.; Huang, F.H. Alkyl Chain Length-Selective Vapor-Induced Fluorochromism of Pillar[5] arene-Based Nonporous Adaptive Crystals. *J. Am. Chem. Soc.* **2019**, *141*, 13290–13294. [[CrossRef](#)]
60. Ju, J.U.; Chung, D.S.; Kim, S.O.; Jung, S.O.; Park, C.E.; Kim, Y.-H.; Kwon, S.-K. Synthesis and characterization of a new ethynyl-linked alternating anthracene/fluorene copolymer for organic thin film transistor. *J. Polym. Sci. Part A Polym. Chem.* **2009**, *47*, 1609–1616. [[CrossRef](#)]
61. Deng, H.Q.; Zhao, E.G.; Li, H.K.; Lam, J.W.Y.; Tang, B.Z. Multifunctional Poly(N-sulfonylamidine)s Constructed by Cu-Catalyzed Three-Component Polycouplings of Diynes, Disulfonyl Azide, and Amino Esters. *Macromolecules* **2015**, *48*, 3180–3189. [[CrossRef](#)]
62. Zheng, C.; Deng, H.Q.; Zhao, Z.J.; Qin, A.J.; Hu, R.R.; Tang, B.Z. Multicomponent Tandem Reactions and Polymerizations of Alkynes, Carbonyl Chlorides, and Thiols. *Macromolecules* **2015**, *48*, 1941–1951. [[CrossRef](#)]
63. Liu, Y.J.; Gao, M.; Lam, J.W.Y.; Hu, R.R.; Tang, B.Z. Copper-Catalyzed Polycoupling of Diynes, Primary Amines, and Aldehydes: A New One-Pot Multicomponent Polymerization Tool to Functional Polymers. *Macromolecules* **2014**, *47*, 4908–4919. [[CrossRef](#)]
64. Li, C.J. Pillararene-based supramolecular polymers: From molecular recognition to polymeric aggregates. *Chem. Commun.* **2014**, *50*, 12420–12433. [[CrossRef](#)] [[PubMed](#)]
65. Gao, Q.Q.; Han, T.; Qiu, Z.J.; Zhang, R.Y.; Zhang, J.; Kwok, R.T.K.; Lam, J.W.Y.; Tang, B.Z. Palladium-catalyzed polyannulation of pyrazoles and diynes toward multifunctional poly(indazole)s under monomer non-stoichiometric conditions. *Polym. Chem.* **2019**, *10*, 5296–5303. [[CrossRef](#)]

66. Zhao, Z.; Su, H.F.; Zhang, P.F.; Cai, Y.J.; Kwok, R.T.K.; Chen, Y.C.; He, Z.K.; Gu, X.G.; He, X.W.; Sung, H.H.Y.; et al. Polyynes bridged AIE luminogens with red emission: Design, synthesis, properties and applications. *J. Mater. Chem. B* **2017**, *5*, 1650–1657. [[CrossRef](#)]
67. Bailey, D.; Seifi, N.; Williams, V.E. Steric effects on [4+4]-photocycloaddition reactions between complementary anthracene derivatives. *Dye. Pigment.* **2011**, *89*, 313–318. [[CrossRef](#)]
68. Belletete, M.; Bouchard, J.; Leclerc, M.; Durocher, G. Photophysics and Solvent-Induced Aggregation of 2,7-Carbazole-Based Conjugated Polymers. *Macromolecules* **2005**, *38*, 880–887. [[CrossRef](#)]